

General Disclaimer

One or more of the Following Statements may affect this Document

- This document has been reproduced from the best copy furnished by the organizational source. It is being released in the interest of making available as much information as possible.
- This document may contain data, which exceeds the sheet parameters. It was furnished in this condition by the organizational source and is the best copy available.
- This document may contain tone-on-tone or color graphs, charts and/or pictures, which have been reproduced in black and white.
- This document is paginated as submitted by the original source.
- Portions of this document are not fully legible due to the historical nature of some of the material. However, it is the best reproduction available from the original submission.

NSA 05-002-134

✓ INFRARED/OPTICAL ENERGY DISTRIBUTIONS OF HIGH REDSHIFTED QUASARS

B. T. Soifer, G. Neugebauer, J. B. Oke, K. Matthews and J. H. Lacy
Palomar Observatory, California Institute of Technology

ABSTRACT

Measurements at 1.2, 1.6 and 2.2 μ m have been combined with visual spectrophotometry of 21 quasars having redshifts $z \geq 2.66$. The primary result of this study is that the rest frame visual/ultraviolet continua of the high redshift quasars are well described by a sum of a power law continuum with slope ~ -0.4 and a 3000 Å bump. The rest frame visual/ultraviolet continua of these quasars are quite similar to that of 3C273, the archetype of low redshift quasars. There does not appear to be any visual/ultraviolet properties distinguishing high redshift quasars selected via visual or radio techniques.

April 23, 1982



(NASA-CR-169436) INFRARED/OPTICAL ENERGY
DISTRIBUTIONS OF HIGH REDSHIFTED QUASARS
(Palomar Observatory) 21 p HC A02/MF A01

N 83-11001

CSCL 03A

Unclass

G3/89 35793

INTRODUCTION

Understanding of the emission mechanisms and underlying energy sources of the visual and ultraviolet continuum in quasars has long been an important goal of quasar observations. The discovery of a significant number of moderately bright high redshift quasars allows a detailed study of the rest frame ultraviolet and visual continuum to be done by observing these objects at visual and near-infrared wavelengths. In this paper we report the results of such a study for 21 quasars having redshifts $z \geq 2.66$.

THE SAMPLE

The objects included in this study were all selected to be moderately bright ($m_v < 20$ mag) quasars with redshifts sufficiently large to bring the Lyman continuum discontinuity into the visual wavelength range. The objects are listed in Table 1. A discussion of the results of the study of the Lyman discontinuity in this sample is found in Oke and Korycansky (1982).

Fourteen objects in the present sample were discovered originally in radio surveys. The remaining 7 were discovered in visual surveys; five of these were discovered in the University of Michigan objective prism survey (MacAlpine and Lewis 1978, MacAlpine, Smith and Lewis 1977). Positions and redshifts for all the objects in this study with the exception of 1320-10 (POX 175; Kunth, Sargent, and Kowal 1981) are found in the catalog of Hewitt and Burbidge (1980). It is clear that the sample observed is not homogeneous; neither the radio nor visually selected samples obey well defined selection criteria.

OBSERVATIONS

All the new observations reported here were obtained on the Hale 5.08 m telescope at Palomar Mountain. The visual observations at observed wavelengths between 3200 Å and 10000 Å, (rest wavelengths between ~ 800 Å and 2500 Å) were obtained with the multichannel spectrometer with band passes of 80 Å below 5600 Å and 160 Å above 5600 Å. These data were reported in Oke and Korycansky (1982). In the case of PKS 0528-253, multichannel observations were not available, and published observations (Smith, *et al.* 1979) were used in the visual range. The infrared observations in the 1.25 μm , 1.65 μm , and 2.2 μm photometric bands were obtained with a solid nitrogen cooled InSb detector. The diameter of the focal plane aperture for all the infrared observations was 5".

The continuum flux densities in the three infrared bands (1.25 μm , 1.65 μm and 2.2 μm) are given in Table 1 for each quasar; at a mean redshift of 3 these correspond to rest frame wavelengths of ~ 0.31 μm , ~ 0.41 μm and ~ 0.55 μm . The observations have been corrected for emission lines in the photometric bands as discussed below and the magnitudes of these corrections are given in Table 2. The flux density at a rest wavelength of 0.174 μm obtained from the multichannel observations is also included in Table 1. In several cases infrared and visual photometry were obtained on several nights for the same object. Except as noted below, the observations agreed within their statistical uncertainties for the objects where multiple observations were obtained, and the flux densities reported represent the average of all observations, weighted by their uncertainties.

In two cases, 0758+12, and 2351-154, the infrared photometry at one or more wavelengths suggests significant variability; in both cases there is evidence for color changes as well. The dates of observations and observed magnitudes at 1.2, 1.6, and 2.2 μm of 0758+12 and 2351-154 are given in Table 3. For 0758+12

the data at $2.2 \mu\text{m}$ indicate variability at the 99% confidence level, while the data at other wavelengths do not show evidence for such variability. For 2351-154 the data at all three wavelengths show strong evidence for variability, with a total variation of 1.5 mag at $2.2 \mu\text{m}$. Indeed it is clear that this quasar varied by $\sim 30\%$ over the one month period of 1981 October/November. In this case there is marginal evidence for a color change with the variation, the $[1.6 \mu\text{m}] - [2.2 \mu\text{m}]$ color changing by 0.4 ± 0.2 mag between 80 July and 81 November.

The infrared continuum observations are affected to some extent by inclusion of strong emission lines in the bandpasses of the observations. The strongest lines in the spectra of quasars that effect the continuum fluxes are $\text{H}\alpha$, $\text{H}\beta$, $[\text{O III}] \lambda\lambda 4959, 5007$, and $\text{Mg II} \lambda\lambda 2800$. Lines weaker than these have small enough equivalent widths to make a negligible individual contribution to the measured continuum level. Of course the sum of weak lines may serve to raise the overall continuum level by a significant amount, but no correction was made for this effect.

For the $\text{H}\alpha$, $\text{H}\beta$, and $[\text{O III}]$ lines, corrections were applied to the observed flux densities assuming the rest frame equivalent width of each line was equal to the average rest frame equivalent width observed in lower redshift quasars (Neugebauer, *et al.* 1979, henceforth NOBM, Soifer *et al.* 1981, and Puetter, *et al.* 1981). The work of Soifer *et al.* and Puetter, *et al.* suggests no strong dependence of hydrogen line strengths on redshift (and hence luminosity). No luminosity dependence has been reported for the strength of $[\text{O III}]$. For $\text{H}\alpha$, $\text{H}\beta$, and $[\text{O III}]$ the rest frame equivalent widths were taken to be 300, 100, and 50 Å respectively. For $\text{H}\alpha$ and $\text{H}\beta$ the line width was assumed to be 10000 km/sec (full width at zero intensity), while the $[\text{O III}]$ lines were assumed to be quite narrow. A correction was made for contributions of the Mg II line in the $1.2 \mu\text{m}$ flux density for quasars having redshifts $z > 3.1$. The maximum correction to the

continuum flux for those quasars affected by the line is expected to be $< 10\%$. This correction is made uncertain by the possible luminosity dependence of the equivalent width of Mg II noted by Baldwin *et al.* (1978). Because of this, a correction was applied only for two quasars, whose rest frame Mg II $\lambda\lambda 2800$ equivalent width is predicted, on the basis of results of Baldwin, *et al.*, to be $\gtrsim 30$ Å.

No attempt has been made to estimate an uncertainty associated with the corrections in Table 2 since the corrections were made for an average quasar emission line spectrum, and there is significant variation within the quasars. Continuum flux densities for wavelengths longer than $\lambda\alpha$ from the multichannel spectrophotometry and infrared photometry corrected for emission line contributions are shown in Figure 1. Where variability is suggested, the energy distribution plotted in Figure 1 is that at a single epoch, with the visual and infrared data separated by the minimum time available. For comparison, the energy distribution of 3C273 (Boggess, *et al.* 1979) over the same rest frame wavelength range is also shown.

DISCUSSION

The quasars observed represent roughly half of those known with redshifts $z \geq 2.66$; thus the results obtained here are probably representative of high redshift quasars as a whole. The high redshift nature of the sample means the quasars in the sample will be of intrinsically high luminosity. Indeed, the two highest luminosity objects in this sample, 0100 + 130 (PHL 957) and PKS 2126-158, are among the most luminous quasars known. Table 4 contains estimates of the luminosity at rest frame wavelengths of $0.17 \mu\text{m}$ and $0.41 \mu\text{m}$. Figure 2 shows histograms of distributions of the luminosities of the present sample. The range in luminosities includes $2.1 < L_U < 34 \times 10^{12} L_\odot$ at ultraviolet wavelengths

($0.17 \mu\text{m}$) and $1.2 < L_0 < 21 \times 10^{12} L_\odot$ at visual wavelengths ($0.41 \mu\text{m}$). In each case the luminosity was approximated by the product $\nu_0 F_{\nu_0}$ where F_{ν_0} is the emitted power density at the rest frequency ν_0 . In this discussion, the wavelengths referred to are, unless otherwise specified, quasar rest frame wavelengths, and the continuum spectral indices and luminosities have been calculated using the flux densities corrected for line emission, as previously described. In estimating these luminosities H_0 was taken to be $50 \text{ km sec}^{-1} \text{ Mpc}^{-1}$ with q_0 taken to be +1; these values were taken for ease of comparison with the results of NOBM.

The observed range in luminosities overlaps the more luminous half of the quasar sample studied by NOBM. The histograms of luminosities (Figure 2) show, however, that many of the quasars in this sample are comparable to or less luminous than 3C273, so the sample studied is not exclusively ultra high luminosity objects. The visually and radio selected quasars span the same range of ultraviolet luminosities; this shows that the limiting magnitudes for the visual searches and radio identification programs are quite similar.

Finally, Figure 2 shows the histogram of the ratio L_{ν}/L_0 , i.e., the ratio of L_{ν} , the luminosity at $0.17 \mu\text{m}$, to L_0 , the luminosity at $0.41 \mu\text{m}$. The mean value of this ratio is 1.6, and in no case is the ratio less than 1.1. Thus, this sample of quasars is indeed a sample of ultraviolet bright quasars i.e., quasars which are more luminous at ultraviolet wavelengths than at other observed wavelengths. NOBM have shown that in many low redshift quasars there is a peak in the power emitted around $3 \mu\text{m}$. It would thus be interesting to study the rest frame infrared properties of the current sample of high redshift quasars to see if a similar peak occurs in these quasars. Unfortunately, current instrumental sensitivities preclude a significant program of such observations.

The continuum shapes displayed in Figure 1 show a wide variety of behavior that is rarely characterizable by a simple power law. Many show a maximum in the continuum between 0.3 and 0.4 μm and have a general convex energy distribution with the slope steepening with increasing frequency. The variety in the observed continua is quite similar to that found by NOBM in the sample of low redshift quasars.

We have attempted to fit the continuum flux densities as the sum of a power law, $f_\nu \propto \nu^\alpha$, "bump" centered at 0.31 μm which represents the 3000 \AA excess that has been previously studied by several authors (e.g., Baldwin 1975, Grandi and Phillips 1980, NOBM, Puetter *et al.* 1982, and Grandi 1982). For this fitting, the multichannel continuum flux densities at rest frequencies corresponding to $\log \nu_0 = 15.17, 15.24, 15.31$, and 15.35, and the infrared observations corrected for the presence of the strongest emission lines were used; the multichannel frequencies were chosen so the continua were free of emission lines. The adopted shape of the 3000 \AA bump was derived from the continuum energy distribution of 3C273 as reported by Boggess *et al.* (1979) by assuming the "bump" was the excess flux over the power law fitted between 5586 \AA and 1600 \AA . The amplitude of the 3000 \AA excess is described by the ratio of f_B , the flux density of the bump, at its peak wavelength 0.31 μm , to f_C , the flux density of the power law component at the same wavelength. This "3000 \AA bump" is clearly the sum of components that have been studied in detail by several authors (e.g., Grandi, 1982; Puetter *et al.*, 1982 and Oke, Shields and Korycansky 1982). The adopted shape agrees well with that found by Oke *et al.* (1982). The best fit parameters of α_{00} and of f_B/f_C are given in Table 4 and histograms of their distributions are given in Figure 3. The uncertainties in the model parameters are roughly ± 0.05 in α_{00} , and ± 0.1 in f_B/f_C .

Eighteen quasars have enough observations to be fitted. For these as a group, the power law plus bump gave a vastly superior fit than the fit with a power law only. For 15 quasars, the model gave statistically satisfactory fits to the observations. For 2126-158, 0805+046 and 0758+12 no simple model gave a satisfactory fit to the observations. In the two cases where the model formally resulted in negative amplitudes for the bump, the bump amplitudes were consistent within the uncertainties with zero amplitude. The success of the simple model suggests that at the resolution of these observations a more complex spectral structure is not required to describe the visual/ultraviolet continua of these quasars.

The mean spectral index from visual through ultraviolet wavelengths of this sample of high redshift quasars is -0.37 ± 0.05 . This mean spectral index is in good agreement with the spectral index $\alpha = -0.5 \pm 0.1$ found by Richstone and Schmidt (1980) for a large sample of quasars with a large range of redshifts. The mean bump to continuum ratio f_B/f_C is 0.30 with a dispersion of 0.20.

From the data of Boggess *et al.*, the spectral index α_{V0} of 3C273 is -0.54 ± 0.05 and the bump to continuum ratio of f_B/f_C is 0.7 ± 0.1 . The spectral index of 3C273 is well within the range of α_{V0} found for the high redshift quasars, while the strength of the bump in 3C273 is somewhat greater than the mean bump amplitude though within the range found for the high redshift sample. The success of the model fits, using the bump excess defined from the 3C273 data, and the fact that the range of parameters derived from the high redshift samples encompasses 3C273 argues that at this resolution the ultraviolet/visual continua of the high redshift quasars are similar to that of 3C273, and by inference to the continua of other low redshift quasars, since 3C273 is archetypical of this class of objects.

Oke and Korycansky (1982) have defined a spectral index α_{UV} between 2000 and 1200 Å, from the observations of many of the quasars of this sample. They find a mean value $\alpha_{UV} = -0.49 \pm 0.04$. There is thus a suggestion of a steepening of the power law continuum at shorter wavelengths. This marginal steepening is significantly less than that derived by Cheney and Rowan-Robinson (1981) from an analysis of the Hewitt Burbidge catalog (1980).

A search was made for correlations between the various parameters of the model fit. None was found. In particular, as shown in Figure 3, there is no correlation between the power law slope and the strength of the bump. It is also seen in Figure 3 that there is no obvious correlation of bump excess with luminosity although Malkan and Sargent (1982) have suggested that the strength of the 3000 Å bump is correlated with luminosity for quasars and other active galactic nuclei.

Eleven of the quasars observed in the present sample have been observed with the Einstein Observatory at X-ray wavelengths by Zamarani, *et al.* (1981) and Ku, *et al.* (1981); five of these, all radio selected quasars, were detected at X-ray wavelengths. For the latter sample of 5 quasars, there is no correlation between α_{VO} and α_{OX} , the visual X-ray spectral index. The mean α_{OX} of these five quasars is -1.81, while the mean α_{VO} of the same quasars is -0.35. Clearly, a significant steepening of the quasar spectra must occur at wavelength shortward of the observed ultraviolet wavelengths. For two cases where high resolution spectra are available, Oke and Korycansky (1982) showed that the steepening did not begin at least until the Lyman jump was reached. IUE observations of the high redshift quasar Q 2204-408 by Wilson, Carnochan, and Gondhalekar (1979) give a spectral index between 1500 Å and 400 Å of -1.5 which suggests a steepening slope below 900 Å. Observations of PG 1115+080 with IUE by Green *et al.* (1980) show a similar effect.

There is no evidence in these observations for different continuum properties among the radio and visually selected quasars in the sample. This is illustrated by the histograms of Figure 3, which show that both radio and visually selected quasars span the full range of spectral index, α_{U0} , and of the bump to continuum ratio f_B/f_C . Thus, to the level at which the visual identification of the radio sample did not introduce a bias in the visual properties of the radio sample, no differences exist in the continuum properties at ultraviolet/visual wavelengths between the radio and visually selected quasars observed here.

SUMMARY

A photometric/spectrophotometric study of 21 high redshift quasars in the observed wavelength range $0.3 - 2.2 \mu\text{m}$ (rest wavelength range $\sim 800 - 5500 \text{\AA}$) has led to the following conclusions:

- 1) The visual/ ultraviolet continuum distributions of the high redshift quasars are fit adequately by a sum of a power law continuum and a 3000\AA "bump" excess similar in shape to that found in 3C273.
- 2) Overall, the high redshift quasars in this sample have very similar rest-frame visual/ultraviolet continuum properties which are similar to those of the archetypical quasar 3C273.
- 3) There is no correlation apparent between the visual/ultraviolet spectral index and the visual/X-ray spectral index for the five high redshift quasars detected at X-ray wavelengths.
- 4) The visual/ultraviolet continuum properties of this sample of quasars show no correlations with selection technique (i.e. radio vs visual selection).

Acknowledgements

We thank J. Carrasco and K. Sellgren for help with the observations. Infrared research at Caltech is supported by grants from NSF and NASA. The research of JBO is supported by NASA Grant NSG 05-002-134.

TABLE 1
Continuum Flux Densities of High Redshift Quasars

Object	Other Name	z	λ_o (μm)				Observation Dates		
			0.174	0.31	-0.41	-0.55	Visual	Infrared	
0044-00	PKS	2.795	-1.10	-1.00 \pm .04	-1.02 \pm .06	-1.21 \pm .12	77 Aug	81 Nov	
0100+13	PHL 957	2.690	-0.04	+0.09 \pm .02	+0.06 \pm .02	-0.07 \pm .02	76 Oct	79 Jul	
0143-015	UM 366	3.14	-0.47	-0.35 \pm .05	-0.31 \pm .03	-0.35 \pm .04	79 Nov	81 Nov	
0143-010	UM 368	3.16	-1.17	-0.94 \pm .12	-0.85 \pm .05	-0.72 \pm .06	80 Oct	80 Oct	
0146+017	UM 141	2.91	-0.44	-0.33 \pm .04	-0.24 \pm .03	-0.26 \pm .04	80 Oct	80 Oct	
0154+045	UM 148	2.99	-0.58	-0.36 \pm .05	-0.27 \pm .03	-0.28 \pm .04	81 Jan	80 Oct	
0207-003	UM 402	2.84	-0.22	-0.04 \pm .05	-0.05 \pm .03	-0.08 \pm .05	80 Dec	80 Oct	
0528-25	PKS	2.765	-0.52	-0.43 \pm .08	-0.28 \pm .04	-0.36 \pm .04	80 Feb	80 Feb	
0642+449	OH 471	3.402	-0.77	-0.53 \pm .03	-0.51 \pm .03	-0.50 \pm .02	73 Apr	73 Dec	
0758+12	MC 5	2.660	-0.94	-0.93 \pm .03	-1.03 \pm .03	-1.17 \pm .04	78 Feb	81 Oct	81 Nov
0805+046	4C05.34	2.877	-0.66	-0.50 \pm .03	-0.43 \pm .03	-0.55 \pm .03	78 Dec	79 Oct	
0830+115	MC 5	2.974	-0.77	-0.71 \pm .04	-0.67 \pm .03	-0.78 \pm .04	77 Feb	81 Nov	
0938+119	MC 5	3.190	-1.31	-1.06 \pm .06	-1.01 \pm .04	-1.20 \pm .09	77 Feb	77 Dec	
0941+261	OK 270	2.910	-0.87	-1.04 \pm .20	-0.72 \pm .04	-0.72 \pm .66	77 Feb	80 Feb	
1004+14	OL 108.1	2.707	-1.00	-0.74 \pm .07	-0.71 \pm .03	-0.77 \pm .04	77 Feb	77 Dec	
1320-10	PKX 175	3.14					80 Feb	80 Feb	
1402+044	PKS	3.202	-1.22				80 Feb	80 Mar	
1442+101	QQ 172	3.53	-0.49	-0.38 \pm .07	-0.47 \pm .04	-0.43 \pm .05	78 Jul	81 Aug	81 Nov
2126-158	PKS	3.270	-0.11	-0.00 \pm .02	+0.0 \pm .02	-0.04 \pm .02	80 Jul	80 Oct	81 Nov
2256+017	PKS	2.663	-0.97	-0.74 \pm .03	-0.80 \pm .02	-0.92 \pm .04	78 Dec	80 Jul	81 Oct
3351-154	OZ 187	2.665		-0.30 \pm .02	-0.27 \pm .02	-0.30 \pm .02	80 Jul	81 Oct	81 Nov

ORIGINAL PAGE IS
OF POOR QUALITY

TABLE 2

Corrections to Observed Flux Densities for Emission Lines

Object	wavelength (μm)		
	1.25	1.65	2.2
	Correction*		
0100+13	--	0.04	0.06 (1)
0143-015	--	--	0.03 (2)
0143-010	0.02	--	0.04 (2)
0528-25	--	0.01	--
0642+449	--	--	0.07 (2)
0758+12	--	0.05	0.12 (1)
0938+119	0.02	--	0.05 (2)
1004+14	--	0.03	0.07 (1)
1320-10	--	--	0.03 (2)
1402+044	--	--	0.05 (2)
1442+101	--	--	0.07 (2)
2126-158	--	--	0.01 (2)
2256+017	--	0.06	0.12 (1)
2351-154	--	0.05	0.12 (1)

*Corrections are $\log \{f_{\nu} \text{ [observed]} / f_{\nu} \text{ [corrected]}\}$

¹corrected for H α in bandpass

²corrected for H β + [O III] 4959, 5007 in bandpass

ORIGINAL IMAGE IS
OF POOR QUALITY

TABLE 3
Photometry of Suspected Variable Quasars

Object	Date	[1.2 μ m]	[1.6 μ m]	[2.2 μ m]
0758±12	02/80	>17.44	17.49±0.18	17.26±0.15
	10/81	17.77±0.11	17.34±0.10	16.66±0.14
	11/81	17.77±0.12	17.53±0.14	16.79±0.19
	χ^2			9.0
2351-154	07/80	>16.88	16.40±0.17	15.84±0.13
	10/81	16.25±0.07	15.59±0.06	14.67±0.08
	11/81	16.12±0.08	15.28±0.07	14.34±0.08
	χ^2		39.9	97.2

TABLE 4

Derived Properties of High Redshift Quasars

 $v_o F v_o$ at $\log v_o =$

Object	Selection Optical/ Radio	z	α_{U0}	f_B/f_C	χ^2/N	α_{ox}	$L_u (10^{12} L_\odot)$	$L_o (10^{12} L_\odot)$	L_u/L_o
0054-00	R	2.795	-0.05	0.32	1.2	<-1.66	2.8	1.2	2.3
0100+13	O	2.690	-0.10	0.42	1.2	<-1.66	31.0	16.0	1.9
0143-015	O	3.14	-0.27	0.29	0.5	<-1.52	14.0	8.6	1.6
0143-010	O	3.16	-0.89	-0.05	0.4	<-1.33	2.8	2.5	1.1
0146+017	O	2.91	-0.43	0.10	1.2	<-1.63	14.0	9.2	1.5
0154+045	O	2.99	-0.57	0.29	1.0	-	10.0	8.9	1.1
0207-003	O	2.84	-0.35	0.36	0.6	-	22.0	14.0	1.6
0528-25	R	2.765	-	-	-	-	11.0	7.9	1.4
0642+449	R	3.402	-0.56	0.36	0.5	-1.19	7.7	6.0	1.3
0758+12	R	2.660	+0.31	0.49	4.6	-	3.9	1.5	2.6
0805+046	R	2.877	-0.31	0.42	2.9	-1.39	8.1	5.9	1.4
0830+115	R	2.974	-0.11	0.29	2.0	<-1.25	6.6	3.5	1.9
0938+119	R	3.190	-0.29	0.79	0.9	<-1.26	2.1	1.8	1.2
0941+26	R	2.910	-0.35	-0.10	1.4	-	5.1	3.1	1.6
1004+141	R	2.707	-0.51	0.58	0.5	-	3.4	2.9	1.2
1320-10	O	3.14	-	-	-	-	-	7.9	-
1402+044	R	3.202	-0.49	0.05	0.6	-1.37	2.5	1.6	1.6
1442+101	R	3.53	-0.23	0.00	0.5	-1.38	15.0	6.9	2.2
2126+158	R	3.27	-0.32	0.24	3.9	-1.22	34.0	21.0	1.6
2256+017	R	2.663	-0.25	0.58	0.7	-	3.6	2.3	1.6
2351-15	R	2.665	-	-	-	-	-	7.7	-

Notes:

All parameters are calculated with correction made for presence of emission lines in photometric band.
 Uncertainties are ± 0.05 in α_{U0} and ± 0.1 in f_B/f_C .

ORIGINAL PAGE IS
OF POOR QUALITY

Bibliography

Baldwin, J. A., 1975, *Ap. J.*, **201**, 26.

Baldwin, J. A., Burke, W. L., Gaskell, C. M., and Wampler, E. J., 1978, *Nature*, **273**, 431.

Boggess, A., *et al.*, 1979, *Ap. J. (Letters)*, **230**, L131.

Cheney, J. E. and Rowan-Robinson, M., 1981, *M. N. R. A. S.*, **195**, 831.

Grandi, S. A., 1982, *Ap. J.*, in press.

Grandi, S. A. and Phillips, M. M., 1980, *Ap. J.*, **239**, 475.

Hewitt, A. and Burbidge, G., 1980, *Ap. J. Suppl.*, **43**, 57.

Green, R. F., Pier, J. R., Schmidt, M., Estabrook, F. B., Lane, A. L., and Wahlquist, H. D., 1980, *Ap. J.*, **239**, 483.

Ku, W., Hefland, D., and Lucy, L., 1980, *Nature*, **288**, 323.

Kunth, D., Sargent, W. L. W., and Kowal, C., 1981, *Astron. & Astrophys. Suppl.*, **44**, 229.

MacAlpine, G. M. and Lewis, D. W., 1978, *Ap. J. Suppl.*, **36**, 587.

MacAlpine, G. M., Smith, S. B., and Lewis, D. W., 1977, *Ap. J. Suppl.*, **35**, 197.

Malkan, M. and Sargent, W. L. W., 1982, *Ap. J.*, **254**, 22.

Neugebauer, G., Oke, J. B., Becklin, E. E., and Matthews, K. (NOBM), 1979, *Ap. J.*, **230**, 79.

Oke, J. B. and Korycansky, D. G., 1982, *Ap. J.*, in press.

Oke, J. B., Shields, G. A., and Korycansky, D. G., 1982, in preparation.

Puettter, R. C., Burbidge, E. M. Smith, H. E., and Stein, W. A., 1982, *Ap. J.*, in press.

Puettter, R. C., Smith, H. E., Willner, S. P. and Pipher, J. L., 1981, *Ap. J.*, **243**, 345.

Smith, H. E., Jura, M., and Margon, B., 1979, *Ap. J.*, **228**, 369..

Soifer, B. T., Neugebauer, G., Oke, J. B., and Matthews, K., 1981, *Ap. J.*, **243**, 369.

Wilson R., Carnochan, D. J., and Gondhalekar, P. M., 1979, *Nature*, **277**, 457.

Zamorani, G., *et al.*, 1981, *Ap. J.*, **245**, 357.

Figure Captions

Figure 1.

The flux densities for high redshift quasars plotted vs rest frequency for each object. The infrared observations are corrected, where necessary, for the presence of the emission lines noted at the top of the figure. Included for comparison is the continuum energy distribution of 3C273. The line through the data for each quasars is the best fit model of a "3000Å bump" and power law continuum as described in the text.

Figure 2.

Histograms of the luminosities and the ratio of luminosities of the sample of quasars at ultraviolet and visual wavelengths. The visually and radio selected quasars are indicated separately, as is the median of the entire sample. The value of the appropriate quantity for 3C273 is also shown in the plots.

Figure 3.

The histograms of α_{U0} , the spectral index and of f_B/f_C , the ratio of the bump flux density to the power law continuum flux density at $0.31 \mu\text{m}$ for the high redshift quasars. The radio and visually selected quasars are indicated separately, and the values of these quantities for the median of the entire sample and for 3C273 are shown in the figure. Also plotted are the ratio f_B/f_C vs spectral index α_{U0} and f_B/f_C vs $\nu_0 F_{\nu_0}$, the luminosity at $0.55 \mu\text{m}$ for the observed quasars. The radio and visually selected quasars are indicated by separate symbols, as is 3C273.

ORIGINAL PAGE IS
OF POOR QUALITY

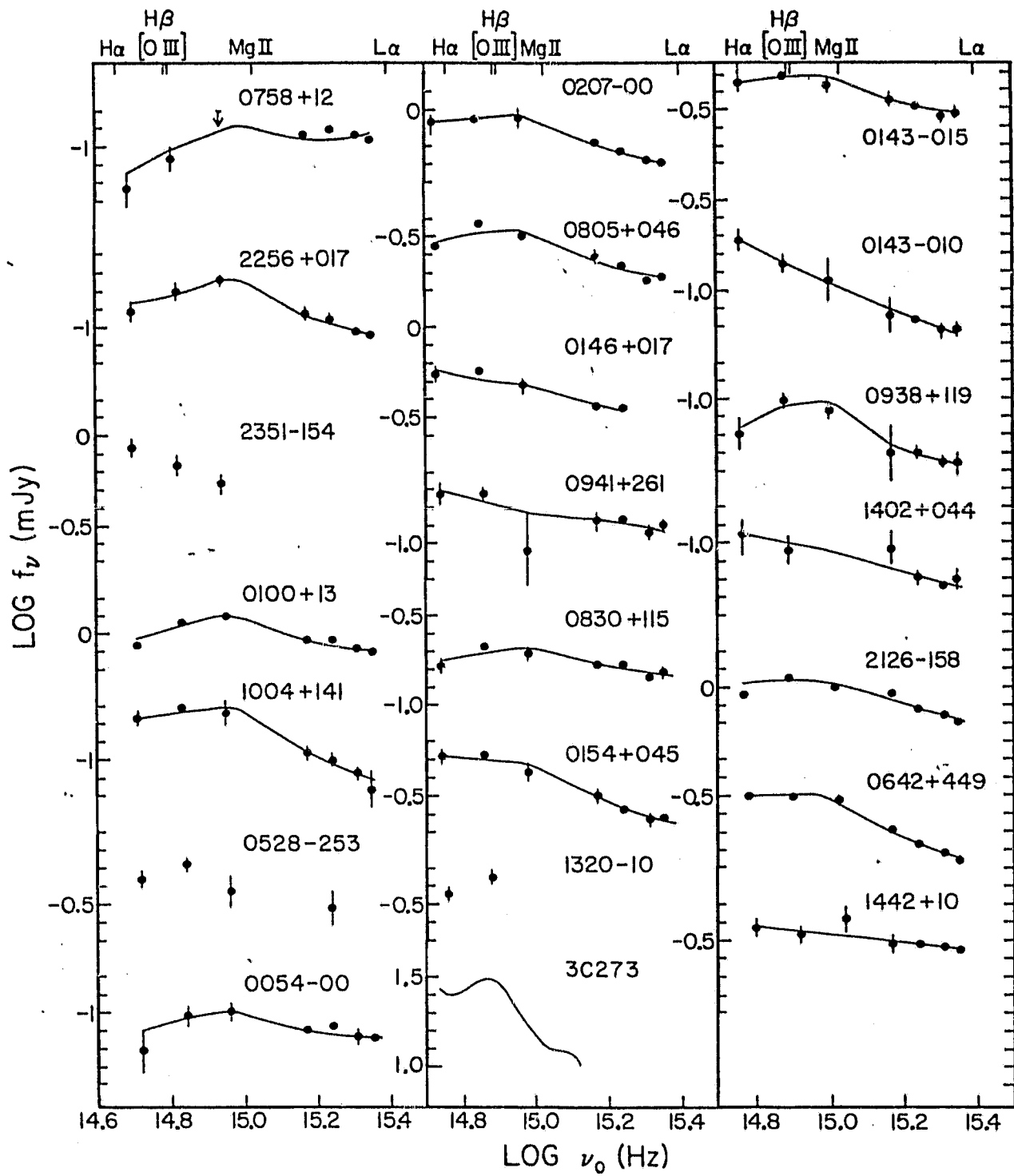


Figure 1

ORIGINAL PAGE IS
OF POOR QUALITY

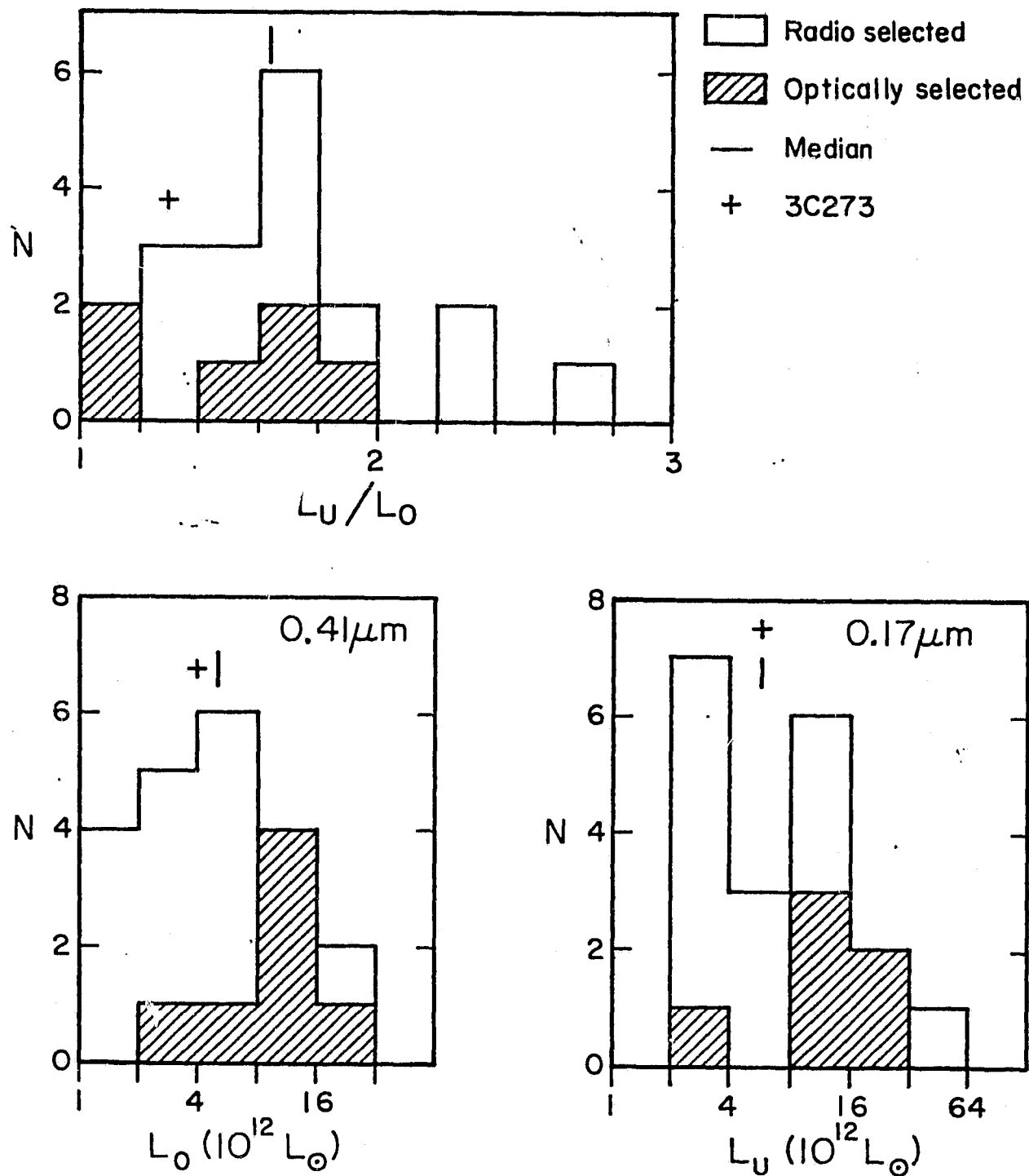


Figure 2

ORIGINAL PAGE IS
OF POOR QUALITY

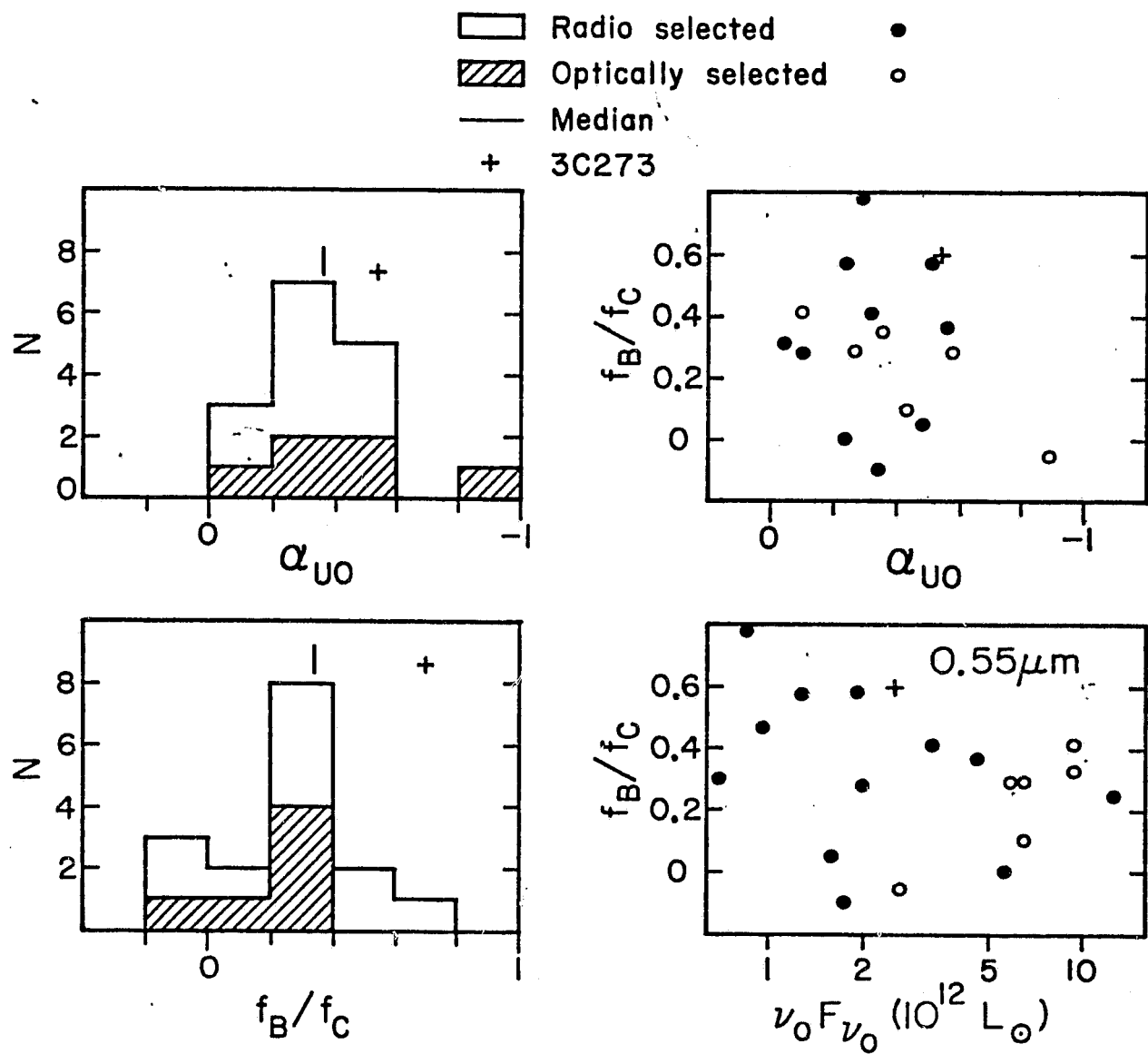


Figure 3